JOURNAL OF NEUROPHYSIOLOGY
Vol. 60, No. 5, November 1988. *Printed in U.S.A.*

Periodicity and Directionality in the Propagation of Epileptiform Discharges Across Neocortex

R. D. CHERVIN, P. A. PIERCE, AND B. W. CONNORS

Department of Neurology, Stanford University School of Medicine, Stanford, California 94305

SUMMARY AND CONCLUSIONS

1. The horizontal propagation of epileptiform discharges has been studied in slices of neocortex treated with high concentrations of bicuculline methiodide, an antagonist of the inhibitory transmitter γ-aminobutyric acid (GABA). The cortical areas examined were: primary somatosensory (SmI) and motor (MI), and primary (area 17) and secondary (area 18) visual areas of rats, and area 17 of cats. In all of these areas an electrical stimulus evoked single, all-or-none paroxysmal field potentials (PFPs) that propagated across the entire width of the slice without decrement.

2. The velocity of PFP propagation was ~0.06–0.09 m/s when averaged over cortical distances of several millimeters. PFP propagation occurred equally well in both directions across a slice.

3. Measurement of PFP propagation at higher spatial resolution (100–180 μm intervals) revealed that velocity was not homogeneous within rat SmI, rat area 18 and cat area 17, but instead varied manyfold as horizontal position changed. In these areas of cortex, propagation patterns were spatially periodic; power spectra reveal that the dominant spatial frequencies were centered about 1 mm^{-1}, with negligible contributions above 2 mm^{-1}. Occasionally PFP propagation was discontinuous, skipping over a small region of cortex and arriving distally before propagating into the more proximal region.

4. In those cortices with periodic propagation patterns, PFP velocity was also strongly direction-dependent. Propagation patterns measured in opposite directions across the same strip of cortex displayed similar periodicities, but in many slices they were negatively correlated, i.e., the propagation pattern in one direction was antiphasic compared to that in the other direction.

5. In contrast, propagation velocity across the center of area 17 of the rat was relatively constant and not directional. Near the boundaries of areas 17 and 18, however, PFP velocity changed abruptly and became periodic within area 18. Similarly, velocity within rat MI was more constant and less directional than in the adjacent SmI.

6. The patterns of PFP propagation velocity are often spatially periodic, directionally asymmetric, and depend upon cortical area. We suggest that the periodic patterns reflect systematic variations in the length or density of horizontal excitatory connections. Alternatively, or concurrently, periodicities could arise from the patchy distributions of intrinsic connections that have been observed anatomically in many areas of neocortex.

INTRODUCTION

Focal seizures arise from large amplitude, abnormally synchronous discharges of cortical neurons (36, 49). Although such discharges may be initiated within a small, discrete area of cortex, they subsequently may spread into large adjacent areas of cortex. The propagation of clinical and experimental epileptiform discharges has been studied at the gross electroencephalographic level (on the scale of centimeters; 24) and, to a lesser extent, at the finer resolution provided by cortical surface recordings in vivo (on the scale of millimeters; 16, 21, 35). However, within the neocortex horizontal propagation has never been measured at a spatial resolution approaching that of single cortical modules, or

columns (on the scale of 100–1000 μm). Columnar systems of the neocortex might be expected to influence the propagation patterns of epileptiform events because of the prominent vertical and horizontal connections associated with them (39).

We have previously studied the initiation mechanisms of experimental epileptiform discharges in neocortex in vitro (6, 7, 17). Epileptiform activity was induced by high doses of γ-aminobutyric acid (GABA) antagonists, which greatly reduce synaptic inhibition. Under these conditions, a small electrical or chemical stimulus can elicit an electrophysiological event that mimics the interictal discharges of epilepsy in many ways: the event is relatively large, essentially all-or-none, reproducible, relatively brief, it has a very variable latency, and it seems to encompass every neuron in a local cortical region. Recorded intracellularly, the discharge is a high-amplitude, prolonged depolarization shift that generates a train of action potentials. Recorded extracellularly in cortical layers II/III, the discharge is prolonged, mostly negative, and has a sharp onset; we have called this event a paroxysmal field potential (PFP; Ref. 6, 7). The PFP provides a convenient measure of the spatial and temporal properties of the synchronized neural activity that underlies the epileptiform activity. Several lines of evidence suggest that this epileptiform event is initiated within neurons of the middle cortical layers and is then propagated vertically to neurons in upper and lower layers (7, 13). Although the subsequent horizontal propagation of the event has previously been noted (17), it has not been studied in detail.

In the present investigation we examine the characteristics of horizontal PFP propagation at a high level of spatial resolution. We have found that the velocity patterns of PFP propagation are inhomogeneous, spatially periodic, direction-dependent, and varying in different histologically distinct areas of cortex. These properties appear to reflect certain anatomic features of intrinsic intracortical connectivity. Some of these results were previously presented in abstract form (8).

METHODS

The techniques for maintaining rat and cat neocortical slices in vitro were modifications of those described previously for guinea pig neocortical slices (9, 31).

Sprague-Dawley rats aged 4–8 wk were deeply anesthetized with intraperitoneal pentobarbital sodium, decapitated, and the brains were removed and placed in cold (~5°C) physiological saline solution. In some of the experiments the barbiturate-anesthetized rat was first cooled to a body temperature of ~25°C by immersion in an icewater bath before removing the brain. A block of cortical tissue was dissected with a scalpel from one of two areas: the parietal region containing primary motor (MI) and somatosensory (SmI) cortex (47), or the occipital region containing primary visual cortex (area 17; striate cortex; Ref. 51) and adjacent secondary visual areas (area 18a and 18b; prestriate cortex). The tissue was then immersed in cold physiological solution.

Cats (aged 2–12 mo) were preanesthetized with intraperitoneal ketamine and then deeply anesthetized with intravenous pentobarbital sodium, and the skull overlying the occipital cortex was removed with a mechanical drill. The animal was then rapidly decapitated, a tissue block containing area 17 was cut from the lateral gyrus, and the tissue was immersed in cold physiological solution.

Tissue blocks were glued to the cutting platform of a vibratome (Lancer Series 1000) and submerged again in cold saline. Rat parietal cortex was cut in either the coronal plane or in a plane generally normal to the cortical surface but running in an anteromedial to posterolateral direction. Rat occipital cortex was cut near the coronal plane, but tilted slightly so that the sections were taken approximately normal to the cortical surface. Cat occipital cortex was cut in the coronal plane, normal to the cortical surface. Single slices from cats contained the dorsal (highly curved) part of the lateral gyrus, and a long, relatively straight area of the medial bank of the same gyrus. Slices were cut to a nominal thickness of 400 μm and transferred to an interface chamber, where they rested on filter paper through which experimental solutions were superfused. The control bath solution contained (in mM): NaCl, 132; KCl, 5; $CaCl_2$, 2; $MgSO_4$, 6; NaH_2PO_4, 1.25; $NaHCO_3$, 26; dextrose, 10; saturated with 95% O_2-5% CO_2 (pH = 7.4). The unusually high Mg^{2+} concentration was used to reduce excitability, thus preventing spontaneous epileptiform activity and its associated spreading depressions. The temperature of the slices was maintained at 34 ± 1°C.

Slices were stimulated electrically with monopolar, sharpened tungsten wires placed in layer VI. Single cathodal shocks of 200-μs duration were delivered through a digitally controlled stimulus isolation unit. Extracellular field potentials were recorded through glass micropipettes (3–7 MΩ) filled with 1 M NaCl and led, via an Ag/AgCl electrode,

to high input impedance preamplifiers. Paired recording pipettes were glued together with epoxy at tip distances of 80–170 μm. Each stimulating and each recording electrode (or each fixed pair of electrodes) was held by an independent micromanipulator. Data were recorded on an Ampex FM tape recorder (0–5 KHz bandwidth) and analyzed off-line using a digital computer.

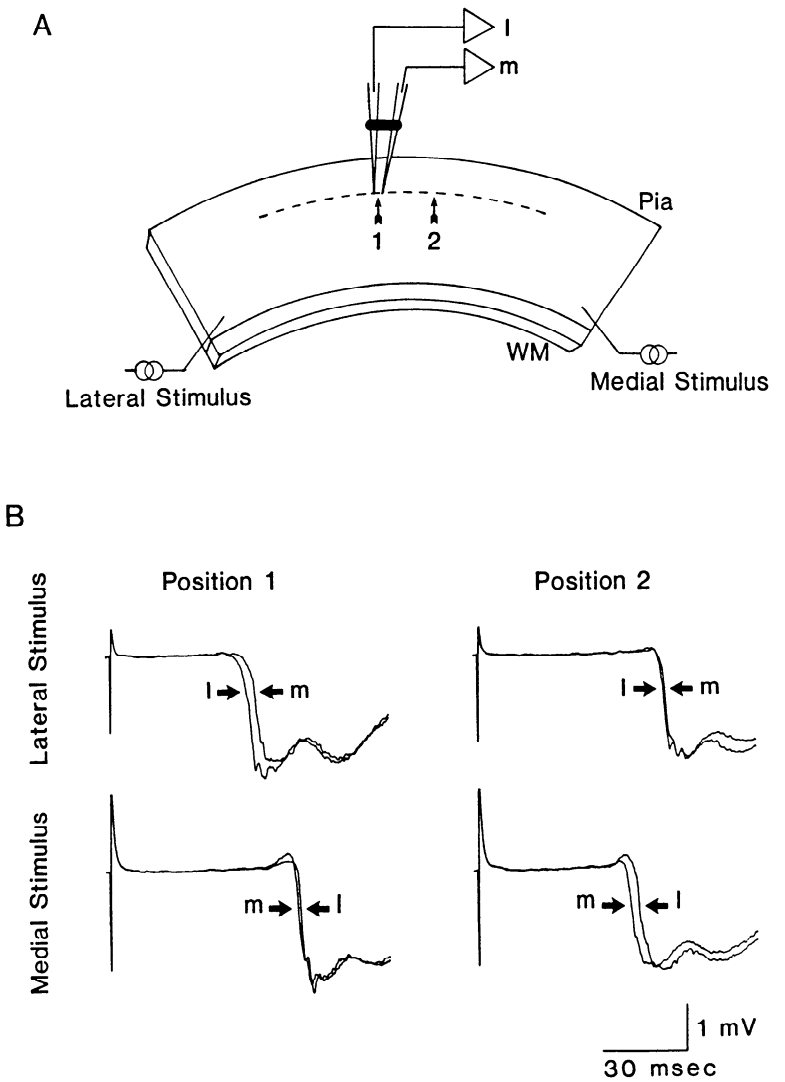

FIG. 1. *A*: schematic diagram of a cortical slice with electrodes situated for stimulating either end and recording (l, m) the PFPs elicited. The 2 recording electrodes were glued together at a fixed intertip distance (80–170 μm). Recordings were made over several millimeters of cortex at regular intervals along a course parallel with the pia (- - -). The stimulus sites were located $\geq$1 mm horizontal to the boundaries of the recording area, to avoid an influence of direct stimulus-evoked activity on propagation. Control experiments showed that changes in stimulus site did not affect propagation under these conditions. WM = white matter; l = lateral; m = medial; 1 = recording position 1; 2 = recording position 2. *B*: pairs of PFPs recorded at 2 different positions in the same slice following either a lateral or medial stimulus. Simultaneously recorded traces from electrodes l and m are superimposed. The initial sharp events are stimulus artifacts. For each experiment, the criterion for arrival of a PFP at an electrode was the time at which the voltage trace crossed a reference voltage (level of *arrows*), which was usually near the point of maximum dV/dt. At position 1, the difference in latency of arrival at the two electrodes was much larger with lateral stimulation (3.05 ms) than with medial stimulation (0.85 ms). At position 2, the latency difference was much smaller with lateral stimulation (0.65 ms) than with medial stimulation (2.85 ms).

Slices were allowed to incubate for at least 1 h before recording commenced. The general health of the slices was then assessed in control solution by recording field potentials in upper layers (II/III) while providing shocks at low frequency (~0.1 Hz) to the deep layers below the recording site. Epileptiform activity was induced by adding 10 μM bicuculline methiodide (Pierce Chemical Co.) to the perfusate. Following equilibration (≥30 min), single shocks at low intensity elicited single PFPs.

For the purposes of this paper, the term "vertical" will refer to the dimension normal to the layers of the cortex (connecting the white matter with the pia), and the term "horizontal" will refer to the dimension parallel to the layers of the cortex (as well as to the pia and white matter) and following the convexity of the cortex as necessary. The standard recording arrangement is schematized in Fig. 1*A*. Two stimulating electrodes were used, one near each lower corner of the slice (in this case labeled "medial" and "lateral"). The positions of these remained fixed for the duration of the experiment, unless otherwise noted. The glued pair of recording electrodes was arranged so that the two tips were always aligned along the horizontal. The pair was moved as a unit in fixed increments (either 100 or 180 μm) along the horizontal. At each recording site 3–5 stimuli were delivered at 0.1 Hz to one of the stimulating electrodes and then to the other. The region of recording was never closer than 1 mm to the vertical line rising from either of the stimulating electrodes, to eliminate effects of inhomogeneity of activation on the propagation of PFPs. Slices were visualized through binocular dissecting microscopes and measurements were made with a reticle and with reference to landmarks such as the pia, the border of the white matter, large blood vessels, and the stimulating electrodes.

Following a series of recordings, small holes or dye marks were made at key reference sites in the tissue (usually the stimulus sites and the lateral edges of the recording area). The slices were fixed in formaldehyde, resectioned on a freezing microtome at 40 μm, and stained for Nissl. Histological determinations of cytoarchitectonic boundaries were made by two or three different observers in each case and were done without knowledge of or reference to the physiological data from that slice. Agreement between independent observations was consistent.

To measure the dominant spatial frequencies of propagation patterns, the data from each individual slice were displayed as a power spectrum. Mean latency difference across the entire distance of measurement was subtracted from each point to remove the zero frequency component. Power spectra were constructed from the fast Fourier transform (FFT; Asystant software, MacMillan Corp.) of the resultant data. Model simulations were done on a Compaq Deskpro 286 personal computer.

RESULTS

As described previously (7), in the presence of 10 μM bicuculline methiodide single shocks to the deep cortical layers or underlying white matter elicited PFPs with the following general characteristics: *1*) they were all-or-none, showing a sharp threshold for initiation, and their size and shape were essentially independent of stimulus intensities above the threshold level; *2*) PFPs had durations of several hundred milliseconds; *3*) the latency to PFP onset could vary greatly, especially when the stimulus was near the threshold level; as stimulus intensity increased, latency-to-onset decreased; and *4*) when triggered at a particular position on the slice, PFPs spread horizontally, without decrement, to the ends of the slice. Unless noted, within each slice PFPs were recorded at a fixed distance from the pia, within the upper aspect of layer II/III. At this level the PFPs were largest and had sharp onsets.

To estimate the average conduction velocity across large horizontal distances, PFPs were evoked at one end of a slice and were recorded with two independently positioned microelectrodes. The first electrode was positioned at least 1 mm horizontal to the site of the stimulation and its position was held fixed. The second electrode was systematically moved horizontally, from the site of the first electrode to successively farther positions 1–3 mm away. Conduction velocity was obtained from plots of the PFP *latency difference* between the two electrodes vs. the *horizontal distance* between them. The best fit lines, which are an estimate of average velocity, were calculated by linear regression (all r values were >0.95). In 12 slices of rat SmI, conduction velocity was 0.063 ± 0.023 m/s (mean ± SD).

The method described above gave reliable and reproducible estimates of conduction averaged over distances greater than ~1 mm. However, it was much less accurate over small distances because of errors in measuring the distance between the two recording electrodes after each repositioning. To estimate PFP velocity with higher spatial resolution, an alternate method was devised. Two

recording electrodes were glued together with a tip separation of 80–170 μm. The distance between the recordings thus did not vary from one measuring site to the next. The interelectrode distance was measured under a microscope both before and after each experiment to verify that it had not changed. Electrodes were arranged as shown in Fig. 1*A* and described in the METHODS. The difference in arrival time of the propagating PFP at the two electrodes was defined as the "latency difference," which is inversely related to velocity and independent of latency shifts in time of initiation at the stimulus sites (see Fig. 1*B*). A propagation profile for a horizontal segment of each slice could then be constructed by measuring latency differences in a series of adjacent positions. As recording electrodes were moved across the cortex the shape of the PFPs remained relatively constant. At a particular recording site the PFPs sequentially initiated from opposite ends of the slice (and thus travelling in opposite directions) also had very similar shapes. In contrast, the latency difference was strongly dependent on both the horizontal *position* (cf. different recording positions in Fig. 1*B*) and the *direction* of PFP propagation (cf. different stimulus sites in Fig. 1*B*).

The latency differences were independent of the precise site of the stimulating electrode when it was moved several hundred microns in either direction, as long as the stimulus site was well outside of the zone of measurement. This indicates that, once initiated, the PFP is a self-regenerative event whose behavior is purely dependent on intrinsic cortical characteristics.

To investigate PFP propagation systematically, graphs of latency difference vs. horizontal position were constructed for different areas of cortex under similar conditions. Figure 2 illustrates the general properties of rat SmI. From lateral to medial across the slice (Fig. 2*A*, ——), the PFP alternately moved relatively slowly (large latency difference), then fast (small latency difference), and then repeated the pattern in a periodic manner. PFP propagation in the opposite direction across the same region of the same cortical slice (Fig. 2*A*, – – –) had a similar periodic pattern, but the two patterns were generally out of phase. Strong periodicities were confined to SmI, the boundaries of which were identified after the experiment by its relatively granular layer IV (11, 47). In the slice of Fig. 2, the boundary between SmI and the agranular area MI fell at 3.2 mm. Conduction through MI was consistently less periodic and direction-dependent than it was in the adjacent SmI, however, the small sampling areas of MI prevented detailed analysis.

Conduction patterns were very stable over time; Fig. 2*A* shows the mean ± 2 SD for the latency measurements at each point for each trial, as well as measurements made ~90 min apart in the same slice (cf. trial 1 and trial 2). Figure 2*B* shows the close correspondence between the superimposed means of trials 1 and 2.

In most slices there were one or more recording sites that yielded consistently negative latency differences (i.e., the PFP arrived at the distal electrode before the proximal one). In the vast majority of these cases, the negative latency difference occurred in only one direction of PFP propagation at a particular site (e.g., Fig. 2*A*; medial-to-lateral propagation at 2.7 mm). Presumably, at sites of negative latency differences the PFP jumped ahead to the area of the distal electrode before propagating (forward or backward) into the region of the proximal electrode.

The dominant spatial frequencies of PFP propagation patterns are best illustrated by the power spectra. As exemplified by Fig. 2*C*, in rat SmI the highest power was usually centered near 1 mm^{-1}, although the resolution of these estimates was limited by the size of our sampling increments.

Figure 3 illustrates two more examples of PFP propagation through rat SmI. Data for Fig. 3*A* were taken at intervals of 180 μm, whereas those of Fig. 3*B* were taken every 100 μm. The latter allowed for greater spatial resolution, at the expense of more time necessary to sample a wide region of cortex. Each slice exhibited strong periodicity and antiphasic directionality. Figure 3*B* also illustrates several regions of unidirectional, negative latency differences.

The prominent periodicities in PFP propagation, with a repeat frequency averaging ~1 mm^{-1}, suggested to us that local variations in cortical structure play an important role. One of the best studied areas of neocortex is area 17 (primary visual cortex) of the cat (28) which has a well documented periodic, or co-

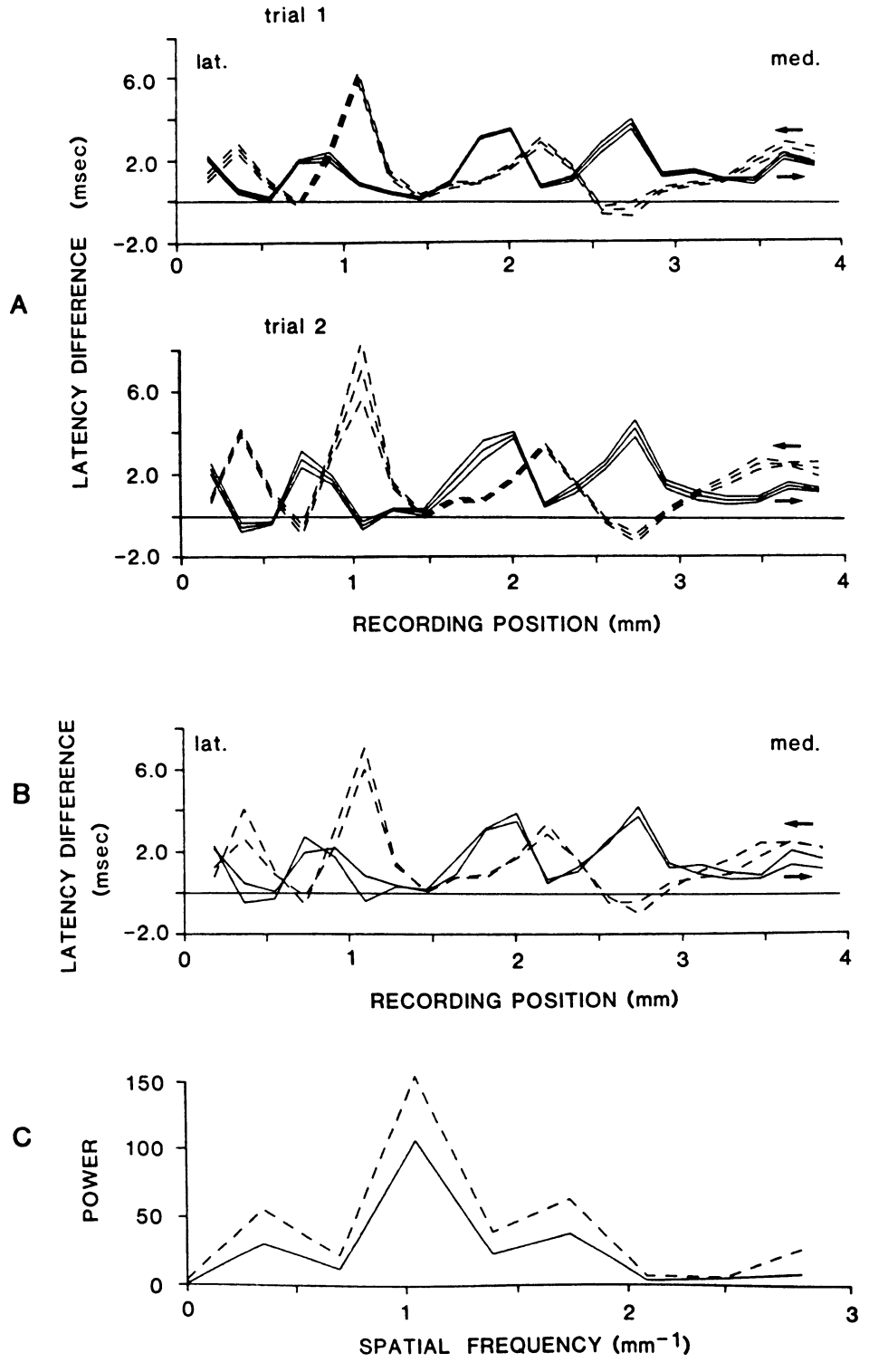

FIG. 2. Spatial variations in PFP propagation across rat SmI cortex. Slice was taken in the coronal plane. *A*: graph of latency differences vs. horizontal position on the cortex for PFPs traveling from medial to lateral (– – –) and lateral to medial (——) over the same slice. Each set of three lines represents the mean of 5 measurements ± 2 SD. Measure-

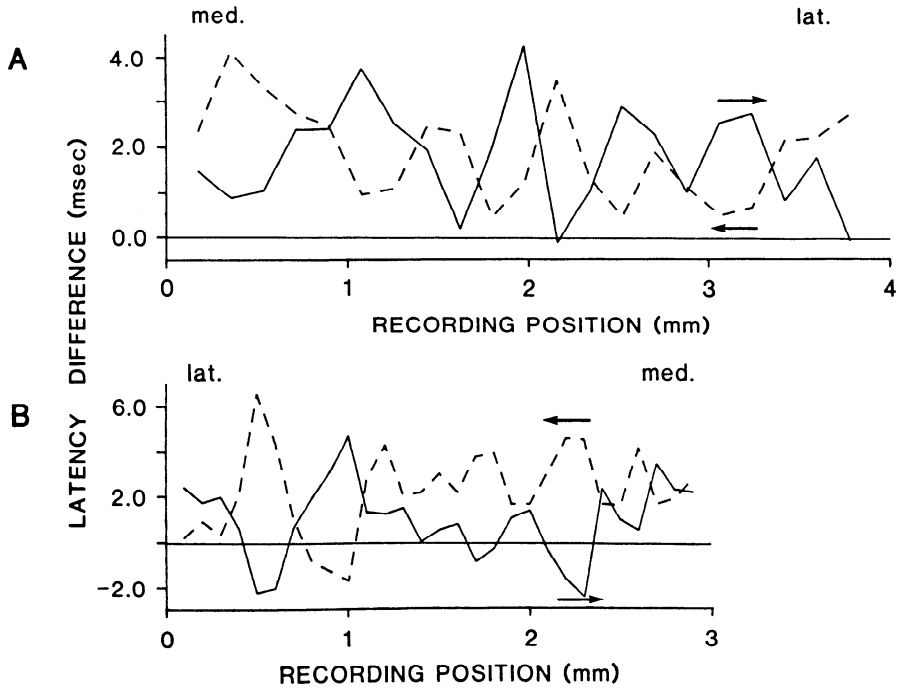

FIG. 3. Further examples of PFP propagation from rat SmI cortex. Data in *A* and *B* taken from slices from different animals. Experimental protocols were the same as described in Fig. 2. The recording intervals in *A* were 180 μm, and in *B* were 100 μm, and the intertip distance of the recording electrodes was 160 μm in *A* and 120 μm in *B*. Each point is the mean of 3–5 measurements.

lumnar, organization with anatomic and physiological correlates. PFP propagation was measured in 4 coronal slices of cat area 17, along the relatively straight medial bank of the posterior lateral gyrus. Measurements were made at 100-μm intervals. As in rat SmI, propagation in cat area 17 was strongly periodic and directional (Fig. 4*A*). Small regions of negative (and unidirectional) latency differences were common (Fig. 4*A*, dorsal-to-ventral at 2.2 mm). When these data were subjected to Fourier analysis, there was a dominant peak at $\sim$1 mm^{-1} (Fig. 4*B*).

Power spectra obtained from individual slices, in particular rat SmI, were somewhat variable in the distribution of their peaks, so the spectrum from each slice was normalized to its peak power and grouped to obtain population characteristics. Figure 5*A* shows the average spectrum (±SD) for 7 slices of rat SmI that were sampled at 180-μm intervals, whereas Fig. 5*B* illustrates the average spectrum from 6 different slices of rat SmI sampled at 100-μm intervals. Both have broad maxima peaking at $\sim$1 mm^{-1}, with significant power extending into lower frequencies. Similarly, spectra from 4 slices from cat area 17 also peak strongly and consistently near 1 mm^{-1} (Fig. 5*C*). The small sample intervals used in the experiments of Fig. 5, *B* and *C*,

ments were made at 180-μm intervals, and the intertip distance of the recording pair was 160 μm. The entire set of measurements was repeated twice, with 90 min intervening (trial 1 vs. trial 2), to test consistency. The data demonstrate periodic variations in the speed of propagation of PFPs as they proceed through the cortex, with a largely inverted pattern for propagation in the opposite direction. Beyond $\sim$3 mm, periodicities became less prominent. Histologically, the region beyond 3.2 mm lacked a distinct layer IV, indicating that it was MI. *B*: mean values from trials 1 and 2 in *A* were superimposed to show the similarities in propagation patterns over time. *C*: power spectrum of propagation data between cortical positions 0 mm and 3 mm from *A*. Relative power is plotted against spatial frequency for data of trial 1 (– – –) and trial 2 (——). Each latency difference was normalized to the average latency difference to remove the zero frequency component.

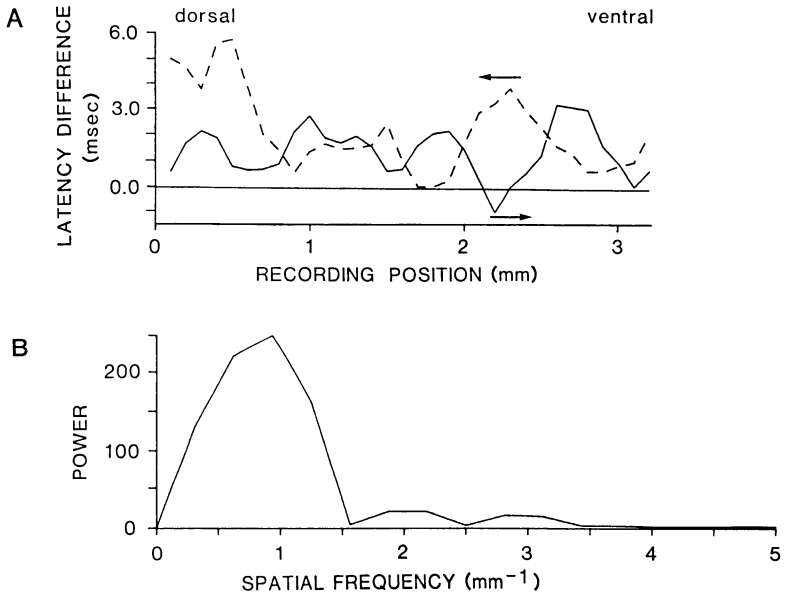

FIG. 4. PFP propagation in cat visual cortex. *A*: latency difference vs. horizontal position for PFPs propagating from dorsal-to-ventral (——) and ventral-to-dorsal (– – –). Slice was taken in the coronal plane from the medial bank of the lateral gyrus. Measurements were made at intervals of 100 μm, and the intertip distance of the recording electrodes was 120 μm. *B*: power spectrum from the data shown in *A*. Peak power occurred near 1 mm $^{-1}$, with negligible power above 1.5 mm^{-1}. Data from the 2 directions were pooled and normalized to the average latency difference.

allow us to conclude that there were negligible components of high spatial frequencies, from >2 mm^{-1} to 5 mm^{-1}, in the PFP propagation patterns.

As a further comparison of cortical areas, we measured PFP propagation in coronal slices of the occipital cortex of rats, cut such that contiguous segments of visual areas 17 and 18 were included. Histological analysis after recording established the areal boundaries based on cytoarchitectonic criteria (51). In 4 such slices, propagation velocity through the central part of area 17 was consistently both aperiodic and independent of direction (Fig. 6, *A* and *B*). However, at a distance of ~200–300 μm from the area 17/18 border, within area 17, latency differences changed sharply. As the PFP propagated into area 18, its pattern became strongly periodic and directional. Recordings from 2 additional slices that comprised area 18 alone confirmed the periodic and directional nature of that region. Data from rat area 18 yielded power spectra with broad single or multiple peaks stretching from 1 mm^{-1} to lower frequencies (Fig. 6*C*, ——); by contrast, analysis of data centered on area 17 (but comprising small segments of area 18 as well, due to the minimum sample requirements of the FFT algorithm used) yielded much lower amplitude spectra with either no clear peak, or a peak at the lowest frequencies (Fig. 6*C*, – – –).

Visual inspection of many of the PFP propagation patterns suggested that, within a slice, the patterns obtained from movement in one direction were 180° out of phase with the patterns obtained from movement in the opposite direction. To quantify this impression, correlation coefficients for the two complete sets of latency differences (one for each direction) in each slice were calculated. As shown in Table 1, a majority of the slices of rat SmI and one-half of the slices of rat area 18 generated significant negative correlation coefficients, whereas data from only 1 of 4 slices from cat area 17 were significant. Correlation coefficients declined when the data from opposite directions were deliberately phase-shifted with respect to one another, indicating that the data are indeed best fit by 180° phase-shifts.

Our method of analysis probably underestimates the extent of antiphasic propagation. In fact, examination of many of the propaga-

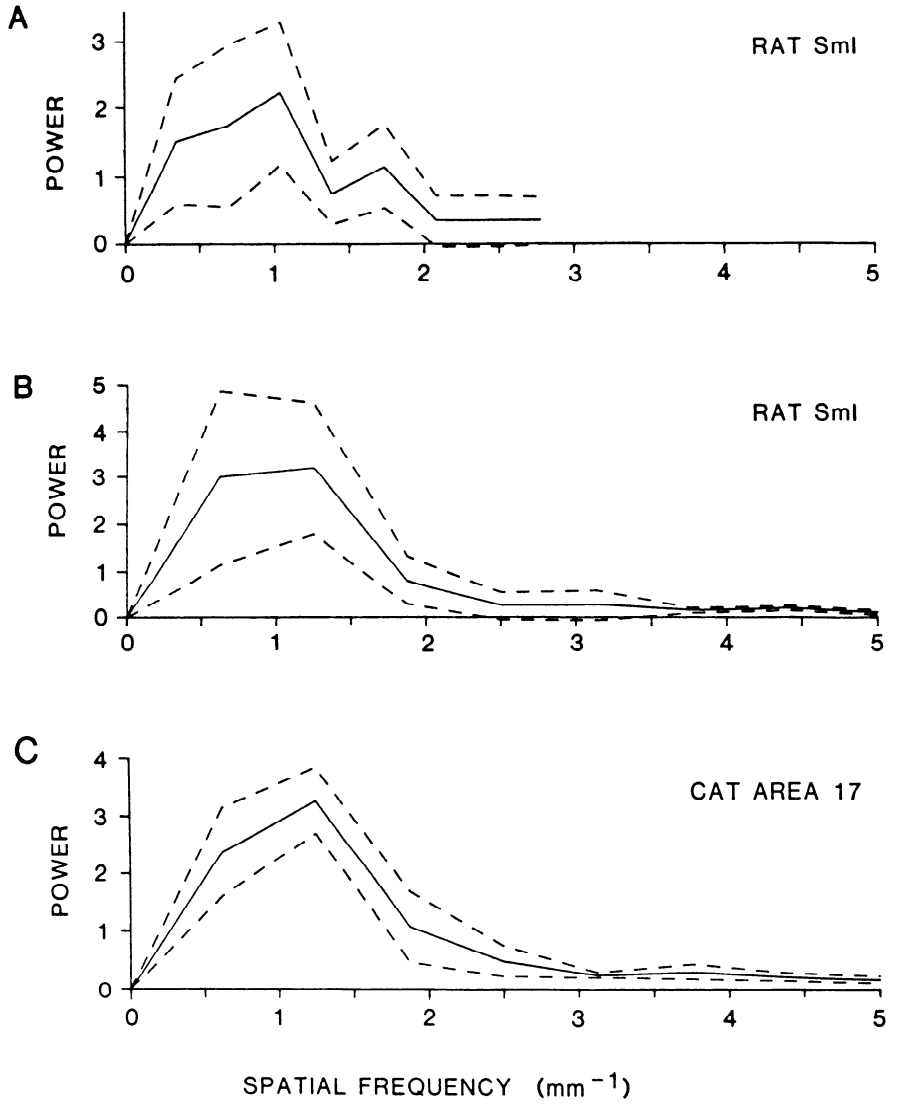

FIG. 5. Averaged power spectra for PFP propagation. Each spectrum from an individual experiment was normalized to its average power across all calculated frequencies, and spectra from all similar experiments were then averaged to generate one spectrum. Each average spectrum is displayed as the mean (——) ± SD (- - -). *A*: spectrum from 7 experiments on rat SmI, with recording intervals of 180 μm. *B*: spectrum from 6 different experiments on rat SmI, with recording intervals of 100 μm. These allow analysis at higher spatial frequencies than in *A*. *C*: spectrum from 4 experiments on cat area 17, with recording intervals of 100 μm.

tion patterns that did not reach statistical significance clearly revealed long subregions of cortex with strongly antiphasic propagation. These slices also had subregions where the antiphasic patterns broke down, and grouping all of the data yielded nonsignificant correlation coefficients. The cat data illustrated in Fig. 4*A*, for example, yielded a nonsignificant correlation coefficient of −0.32, but there are subregions (e.g., from 1.4 to 3 mm) of obvious negative correlation. We conclude that in many regions of rat SmI and area 18, and cat area 17, propagation in one direction is antiphasic with that in the other.

Estimates of the average velocity of PFP propagation across large (several millimeters) lengths of cortex were calculated by dividing the interelectrode distance by the mean la-

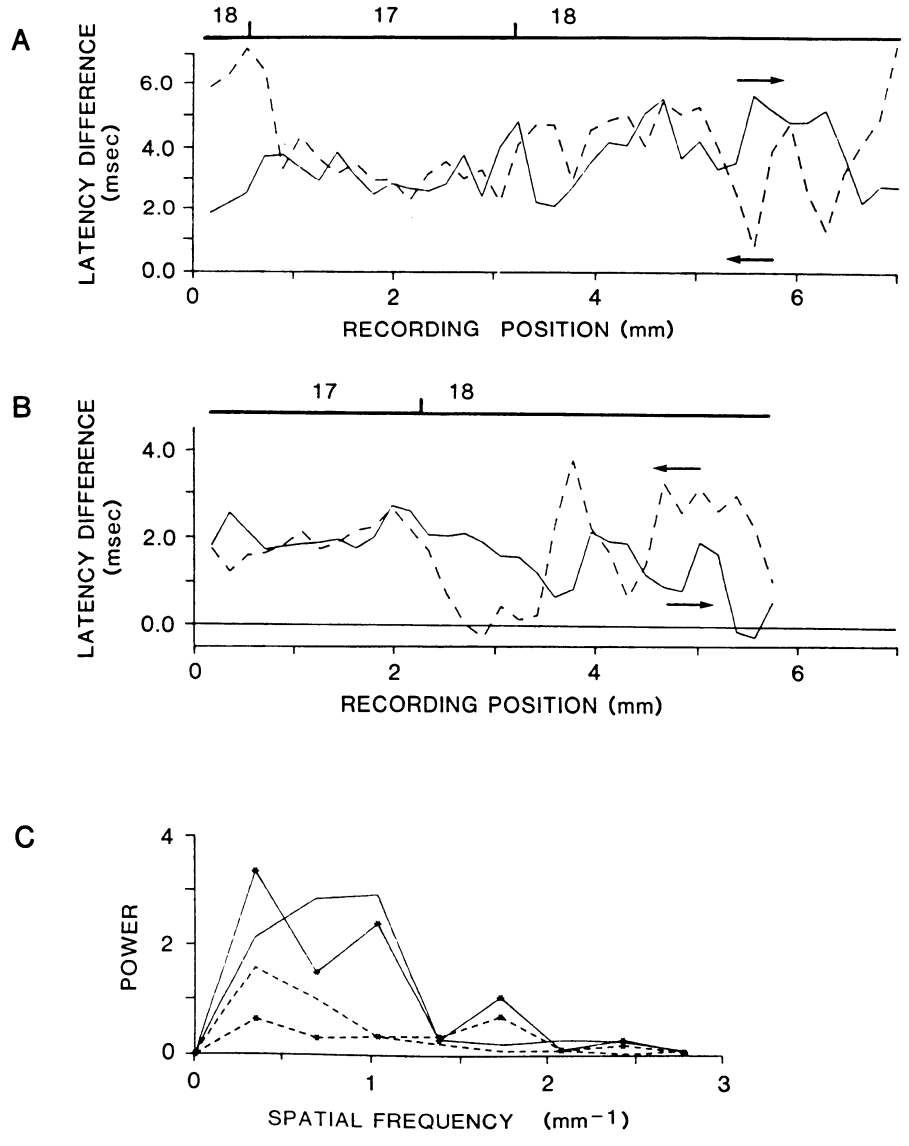

FIG. 6. PFP propagation across rat visual cortex. *A* and *B*: propagation through area 17 is relatively homogeneous and nondirectional, whereas propagation through area 18 is periodic and direction-dependent. The 2 examples were from different animals. Slices were taken in a coronal plane through the occipital pole, medial is to the left. Propagation was from medial-to-lateral (——) and lateral-to-medial (– – –). Measurements were made at 180-μm intervals; the average of 3 to 5 measurements per point is plotted. The borders of areas 17 and 18, determined by histology, are shown by the *heavy lines* above each graph. The intertip distance of the recording electrodes was 150 μm in both cases. *C*: power spectra derived from data shown in *A* and *B*. Each spectrum was generated from 16 points on the graphs of *A* and *B*. Spectra from points centered on area 17 (– – –) show much less power than those encompassing the lateral aspect of area 18 (——). *Starred data* are from *B*, *unstarred data* are from *A*.

tency difference (for all data points from a given direction in each slice). There were no significant or consistent differences between the values obtained for opposite directions in the same slice, so these were grouped. Table 2 summarizes the results, and shows that mean PFP velocity was 0.063 to 0.088 m/s, with the rat visual areas slightly slower than both rat SmI and cat area 17.

All of the measurements described above were obtained from recordings made in layer II/III. To test the laminar specificity of PFP

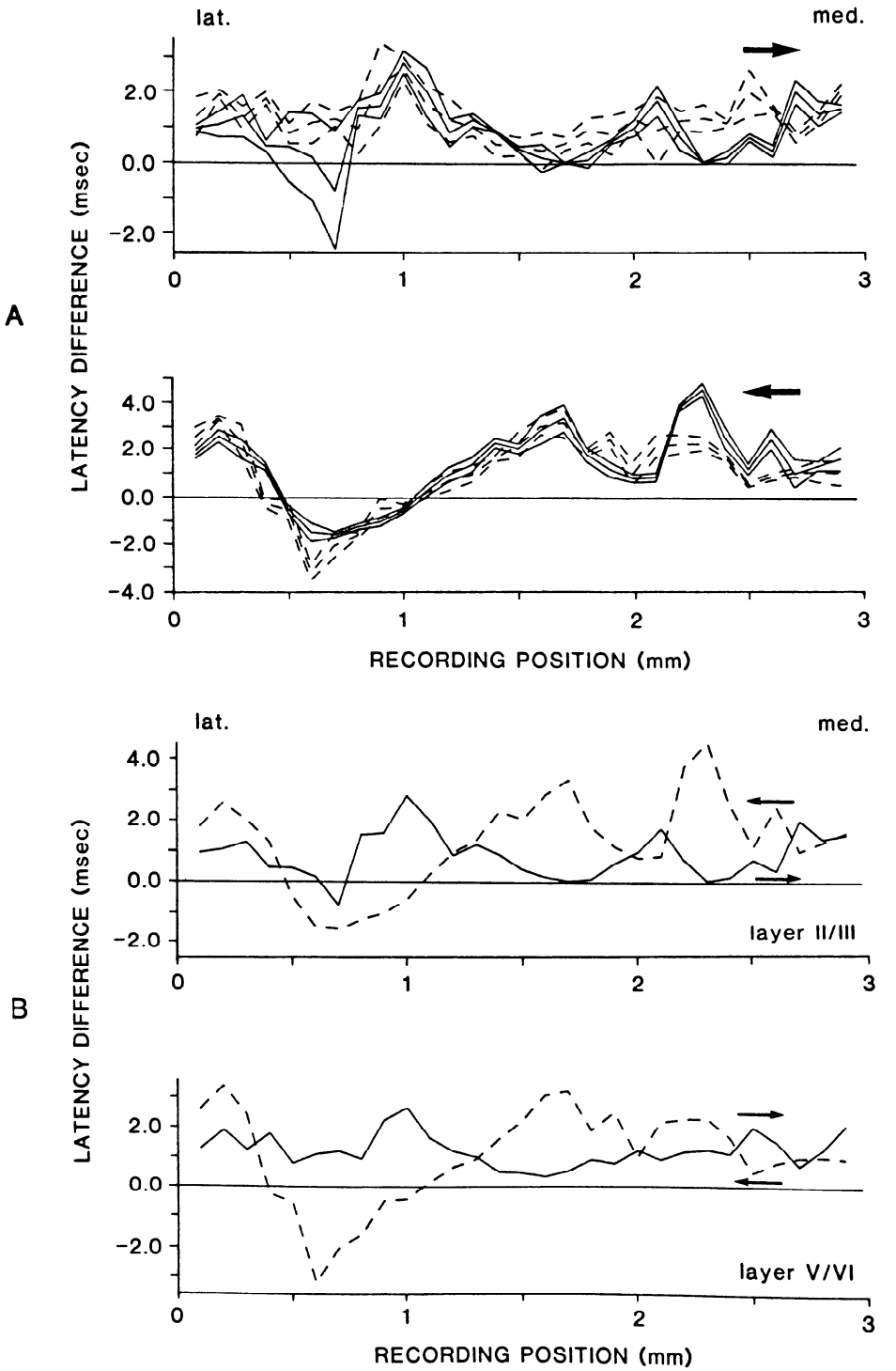

FIG. 7. PFP propagation in deep layers is similar to that in upper layers. *A*: experiment performed as described in Figs. 1 and 2 on rat SmI cortex, with the addition of a set of latency difference recordings along a line near the border of layers V and VI. The *upper graph* plots PFP propagation from lateral-to-medial, measured in layer II/III (——) and layer V/VI (– – –). The lower graph plots propagation from medial-to-lateral, measured in the same way. Each set of plotted lines is the mean ± 2 SD of the latency differences. *B*: means of the same data shown in *A*, rearranged to superimpose data from layers II/III (*upper graph*) and layers V/VI (*lower graph*). The largest variations in upper layer propagation are mimicked in deeper layers, though some flattening of the patterns is evident.

propagation patterns, we made parallel measurements along the usual horizontal line in layer II/III and along a line at approximately the layer V/VI border. To compensate for the convexity of the cortex, measurements in the lower layers were made at shorter horizontal intervals than those in the upper layers; care was taken to line up each upper layer recording site with the corresponding recording site lying along the vertical line in the lower layers. The horizontal positions for each pair of recordings (upper and lower) were considered to be the distances measured in the upper layers, although the lower recordings covered a smaller absolute distance. Figure 7 illustrates results from such an experiment in rat SmI. Figure 7*A* shows the superimposed patterns obtained from the lateral-to-medial direction (*top*) and the medial-to-lateral direction (*bottom*) recorded in the upper layers (——) and lower layers (– – –). Figure 7*B* shows the means of the same data rearranged so that the bidirectional patterns from the upper layers are on top and those from the lower layers are on the bottom. The patterns from upper and lower layers show strong similarities, and the most prominent features (e.g., the long latency peak at 1 mm in the lateral-to-medial direction, and the unusually large and wide area of negative latencies in the medial-to-lateral direction at 0.6 mm; Fig. 7) are reproduced in both upper and lower layers. Many of the smaller amplitude variations evident in the upper layers were not clearly visible in the lower layers, however. The PFP appears to travel across all layers at the same velocity, when averaged over millimeters (thus it moves horizontally as a relatively constant wave front in the vertical dimension), but there may be short distances within which the upper layers lag or lead the deeper ones.

TABLE 1. *Correlation coefficients for oppositely directed propagation patterns*

Cortical Area	No. Significant/ Total Slices	Mean $r \pm$ SD for Significant Slices	Significance Level
rat SmI	8/13	-0.55 ± 0.12	$P < 0.02$
rat area 18	3/6	-0.62 ± 0.20	$P < 0.01$
cat area 17	1/4	-0.48	$P < 0.003$

The correlation between all PFP latency differences from propagation in one direction vs. all those from propagation in the opposite direction were calculated for each slice. Correlations were listed as "significant" if the P value was <0.05; of these, the least significant P value was actually 0.02. The last column lists the least significant P level for each group.

TABLE 2. *PFP propagation velocities for various cortical areas*

Cortical Area	Conduction Velocity, m/s	No. of Slices
rat SmI	0.088 ± 0.019	14
rat area 17	0.063 ± 0.017	4
rat area 18	0.065 ± 0.023	6
cat area 17	0.085 ± 0.018	4

Conduction velocity for each slice was calculated by dividing the distance between the recording pair of electrodes by the mean latency difference. Velocities are given as means ± SD.

DISCUSSION

The primary conclusions of this study are that the horizontal propagation of a neocortical epileptiform event, the PFP, has several characteristics: *1*) velocity in several cortical areas is not uniform but instead shows a *spatially periodic* pattern, with dominant frequencies of ~ 1 mm^{-1}; *2*) velocity is very *direction-dependent; 3*) patterns of propagation in opposite directions across the same region of cortex are often *phase-inverted*; and *4*) different architectonic areas of cortex consistently display different propagation patterns.

There have been few detailed studies of the horizontal propagation of either clinical or experimental epileptiform discharges through the neocortex. Petsche et al. (35) reported that both the pathway and speed of propagation of repetitive seizure events in an intact rabbit penicillin focus were very irregular. Goldensohn and Salazar (16), using data averaged over many cats and several millimeters of cortex, estimated a propagation velocity of 0.25 m/s for an epileptiform event around a penicillin focus in vivo. It is hard to draw direct comparisons between these studies and ours. Experimental constraints in vivo prevented spatial analysis at resolutions below 1–2 mm, steep gradients of drug concentration around the focus may have spuriously influenced propagation, and possible effects of subcortical connections cannot be determined.

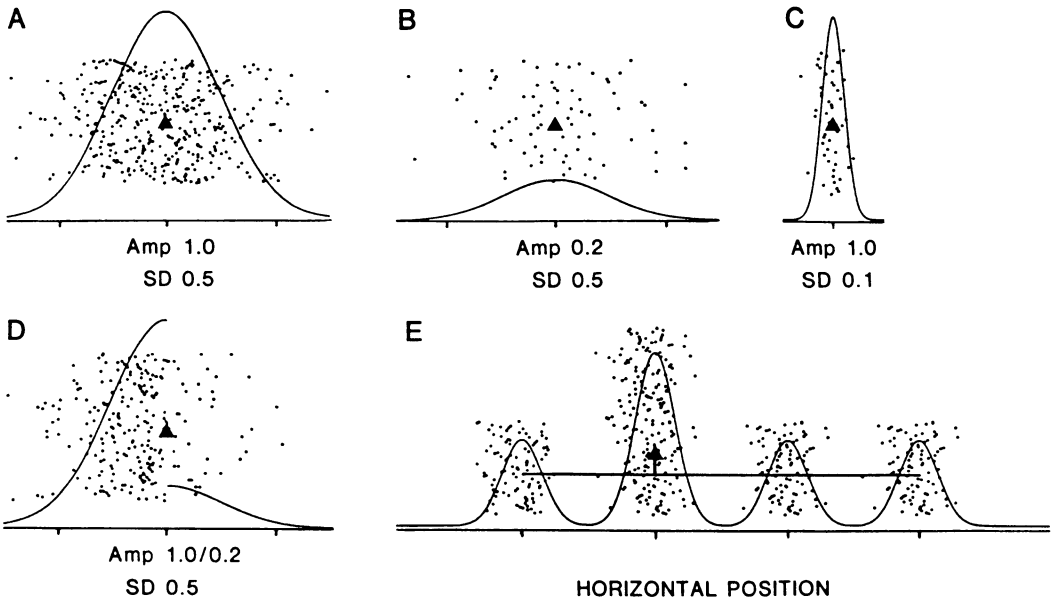

FIG. 8. Schematic illustration of possible variations in patterns of local intracortical connections. *A*: simple Gaussian distribution of synapse density (*solid curve*) as a function of horizontal distance from the originating cell bodies (represented along the *abscissa*). Maximal density is set to 1.0 (Amp) and SD is 0.5. The same synapse distribution is also schematically illustrated by the density of dots at varying horizontal distances from the central position of the somata (▲). The vertical position of the dots is random. *B*: same as in *A*, except that the peak synapse density has been reduced to 0.2 while keeping SD constant. *C*: same as in *A*, except that the SD has been reduced to 0.1 while keeping the peak synapse density constant. *D*: asymmetrical distribution of synapse density, with high density in leftward projection (Amp of 1.0) and low density in rightward projection (Amp of 0.2); SD is constant in each at 0.5. *E*: schematic representation of patchy distribution of synapse density. One centrally located set of neurons (▲) generates a high local density of synapses as well as several distantly located, but smaller, sets of synapses, with intervening regions nearly devoid of synapses.

Recently Gutnick and Wadman (18), using a different measurement technique, obtained results similar to some of our own in slices of guinea pig parietal cortex treated with picrotoxin; discontinuities of PFP propagation occurred at intervals of ~0.4–0.8 mm, but they reported no direction-dependence. In contrast to PFPs from slices of neocortex, propagation of epileptiform bursts across hippocampal slices (from an initiating site in CA2 through CA3) was reported to be "smooth and uniform," with an average velocity of 0.13 m/s (23).

Periodicities of propagation

Strongly periodic propagation was observed in areas SmI and 18 of the rat, and area 17 of the cat. Spectral analysis revealed that, despite the widely variant species and functions, the dominant spatial frequencies in each of these areas were broadly centered about 1 mm^{-1}. An obvious question to ask is, what is the anatomical basis for this physiological phenomenon?

In the primary visual cortex of the cat, the periodicities of propagation are similar to the periodicities of the columnar systems for ocular dominance (~800 μm; Refs. 26 and 40) and orientation selectivity (~1.1 mm; Refs. 19 and 25). Rat SmI also has a very prominent form of vertical (or columnar) organization, but one that is quite different from that of cat area 17: the *barrels*, which are dense cylindrical aggregations of small neurons in layer IV (47). It is not clear, however, whether there is any correlation between barrels and PFP propagation patterns. Despite extensive histological efforts, we were not able to find any consistent correspondence between discontinuities in the density of layer IV and the periodicities in propagation within the same slice. One problem is technical; the thickness of a slice in vitro (nominally 400 μm) is large enough to contain whole barrels, parts of barrels, and extensive overlap of barrels. Thus a narrow vertical strip of an SmI cortical slice might actually comprise fragments of more than one barrel or interbarrel region. The

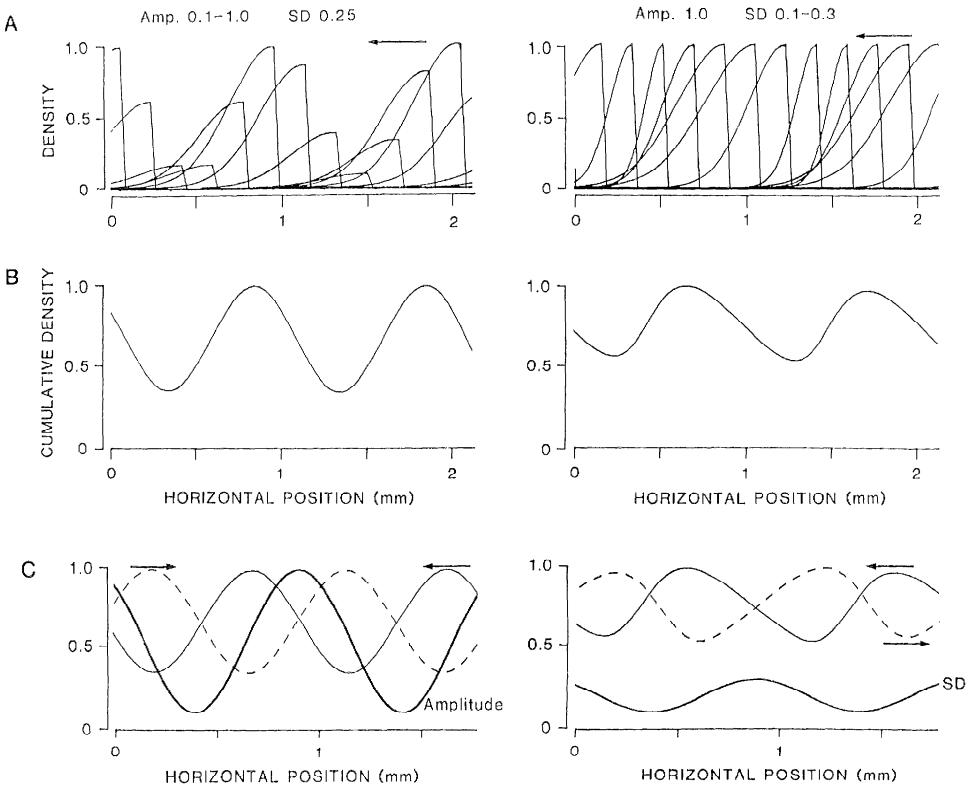

FIG. 9. Simulation of a model of periodic synapse distribution. See text for details. *A*: horizontal density distributions of synapses projecting *only* from right to left. Each half-Gaussian distribution (see Fig. 8*A*) is illustrated at 180-μm intervals and represents the synaptic distribution emanating from one vertical strip of neurons. Note that the model actually used an interval of 60 μm between neuronal groups for all calculations. In the *left graph* the SD of each distribution is kept constant at 0.25, whereas the peak amplitude varies from 0.1 to 1.0 as a sinusoidal function of horizontal cortical position. In the *right graph* the peak amplitude is kept constant at 1.0, whereas the SD varies from 0.1 to 0.3 as a sinusoidal function of horizontal cortical position. *B*: smoothed cumulative density distributions obtained by summation of individual density distributions arranged as in the graphs in *A* above, but spaced 60 μm apart. The *left graph* plots the cumulative distribution for the case in which only amplitude varies; the *right graph* plots the cumulative distribution for the case in which only SD varies. *C*: summary of results for both directions of propagation. In the *left graph* the *thin solid line* repeats the cumulative density distribution shown in *B*, left, for propagation from right-to-left. The *dashed line* shows the cumulative density distribution resulting from connections from left-to-right, which are 180° out of phase with those in the opposite direction. The *heavy solid line* plots the sinusoidal function used to describe the amplitude variations across the cortex; it is 90° out of phase with the cumulative density distributions. The *right graph* summarizes results from the case in which SD was varied. Notation is analogous to that for the *C, left*; in this case the *heavy solid line* represents the sinusoidal function used to describe SD variations. A similar phase relationship is evident.

scaling of the barrel system does not correspond closely to that of the PFP periodicities. Center-to-center spacing of even the largest barrels is no more than ~0.5 mm in the rat, whereas that of the PFP periodicities was most often ~1 mm. It is possible that the propagation patterns correlate with some multiple of the barrel periodicities, or with some other columnar system of rat SmI that overlays the barrels, but such conclusions await additional experiments.

Of the several cortical areas we tested, only the central part of area 17 of the rat clearly displayed uniform and nondirectional PFP propagation. Area MI of the rat also had relatively constant propagation characteristics, but the distances tested were too small to draw firm conclusions. The fact that at least one area of cortex did not show periodicity and directionality implies that these characteristics cannot be explained simply as an artifact of our method of measurement. Indeed, within single slices of rat occipital cortex the PFP consistently displayed very different

propagation patterns within area 17 as compared to the adjacent area 18. The few physiological investigations of rat and mouse area 17 have not reported any obvious columnar system of ocular dominance or orientation (12, 41, 48); however, the inherent technical difficulties of studying such small regions of cortex may have obscured them. It is possible, for example, that in both the studies of receptive fields and of PFPs a relatively high spatial frequency might have gone undetected. In our case, the periodicities would have to be smaller than ~200 μm to escape measurement, because this was about the detection limit of our most fine-grained experiments.

Mechanisms of propagation

What mediates horizontal propagation of the PFP? The most likely candidates are the horizontally directed axons from excitatory neurons (pyramidal cells and perhaps spiny stellate cells). Anatomic studies imply that these types of connections are extensive and ubiquitous in neocortex (1, 3, 5, 14, 20, 22, 27, 29, 32, 37, 38) and arise from neurons of all cellular layers. Lateral excitatory influences have also been demonstrated physiologically (2, 42). Further, the epileptiform events that underlie the PFP arise largely from strong excitatory synaptic currents. Intracellular recordings imply that the majority (perhaps all) of the neurons in the slice display a large depolarizing wave and a concurrent burst of action potentials during the epileptiform event (7, 17, 31). Although it has not been studied in detail, it appears that the sharp negative onset of the PFP in upper cortical layers correlates with the initial action potential of the epileptiform burst in pyramidal cells (Connors, unpublished observations; cf. Figs. 1*A* and 3*A* in Ref. 7). Thus for each recording electrode, our measurements probably estimate the population-averaged time at which the epileptiform burst reaches action potential threshold in the region near the electrode tip.

Alternative mediators of PFP propagation are less likely. Extracellular accumulation of an excitatory substance, such as potassium ions, is limited by constraints of passive diffusion and thus occurs too slowly to account for the observed velocities (cf. Ref. 50), and in any case could not explain the occasional jumps of the PFP across small regions of cortex. Strong ephaptic interactions between neocortical pyramidal cells have not been demonstrated. We suggest that the PFP moves from one vertical strip of cortex to the next via the influence of excitatory synaptic connections in the horizontal dimension.

Mechanisms of periodicity and directionality

What accounts for the periodicity and directionality of PFP propagation? Subcortical influences are ruled out because they have been removed by the slicing procedure. Spatial nonuniformities in local inhibitory circuitry could, in principle, lead to nonuniformities in propagation. However, high doses of bicuculline methiodide block most of the $GABA_A$ receptor-mediated inhibition (10), and indeed no obvious inhibitory postsynaptic potentials (IPSPs) have been observed in pyramidal cells under the conditions used here (17; Connors, unpublished observations). The long-duration, bicuculline-insensitive IPSP of neocortical cells is relatively quite weak and slowly activating (9, 10), and thus it seems likely that it does not influence PFP propagation (cf. Ref. 44). Another possibility is that spatial variations in the intrinsic membrane properties of cortical neurons might lead to periodic differences in excitability across the cortex. A relatively excitable region, due for example to a higher density of intrinsically bursting neurons (9, 31), might reach threshold for PFP initiation more quickly than adjacent areas. However, this scheme cannot readily account for the directionality of the PFP propagation. A more likely possibility is that the patterns of PFP propagation are generated by patterns in the excitatory horizontal connections themselves.

Anatomic investigations show that intrinsic cortical connections may vary greatly in their horizontal extent, density, symmetry, and patterns. The marker horseradish peroxidase (HRP), when applied by focal extracellular injection, labels two prominent systems of ipsilateral cortical connections: *1*) a dense local network of axons and terminals spreading horizontally, in a continuous fashion, from the injection site to immediately adjacent areas, within a variable radius from ~200 μm to >1 mm; and *2*) many longer connections (up to several millimeters) that exhibit discontinuous, or patchy, distributions. For example, in the primary visual cor-

tex of tree shrews and primates, patches are evenly separated by ~350–600 μm (3, 37, 38). Within cat area 17, reconstructions of single HRP-filled pyramidal and spiny stellate cells, the primary excitatory neurons of the cortex, have shown individual cells projecting to discrete patches of cortex (14, 15, 22). Extracellular tracer studies in this cortex also demonstrate a strong system of patchy connections, and in adult cats the interpatch distances average ~800–900 μm (27). Most of the interpatch connections made by pyramidal cells in the cat terminate in asymmetric synapses onto the spines of other pyramidal cells, suggesting excitatory interactions (14, 22, 32). The physiological evidence supports this. Cross-correlation of neuronal firing implies a high degree of excitatory interconnectivity within and between columns of like orientation and ocular dominance (45; however, cf. Ref. 30).

Patchy connections also appear in rat cortex, as shown by HRP studies in frontoparietal areas (20) and by axon degeneration studies in sensorimotor areas (1). Recent tracer studies of rat SmI by Chapin et al. (5) are of greatest relevance to our results, and demonstrate both short- and long-distance corticocortical connections. Over the short range, near the site of tracer injection, horizontal connections spread into supra- and infragranular layers of adjacent granular zones. Over the longer range, there are dense reciprocal connections between the "dysgranular" and "perigranular" zones, i.e., those areas interspersed between the thalamic recipient "granular" zones. Unfortunately, none of the cited studies in rats has systematically quantitated the distances between interconnected patches; however, examination of the published data suggests that distances in the range of 0.5–1.5 mm are most common.

A model of PFP propagation patterns

We have developed a simple model of cortical interconnectivity that may account for some of the periodic and directional patterns of PFP propagation. It incorporates only the local, nonpatchy connections of the *first* type described above. Although the model is rudimentary, it is hard to justify constructing a much more detailed and specific model since the necessary parameters have not been quantified for any neocortical area. In contrast, extensive experimental work on the somewhat simpler circuitry of the hippocampus (e.g., Ref. 33) has allowed some very explicit modelling of epileptiform initiation and propagation (43, 44).

We have made several simplifying assumptions: *1*) only excitatory neurons contribute to the propagation patterns, *2*) neurons of all cortical layers are lumped together, and *3*) the density of cortical synapses emanating from each vertical strip of cortex (along the single horizontal dimension) is assumed to be continuous, symmetrical, and a simple Gaussian function of distance from the originating cell bodies. Thus three parameters completely describe the spatial distribution for each local subset of neurons: the horizontal *position* of the somata, the *amplitude* of the peak synaptic density (which occurs at the position of the somata), and the *standard deviation* (SD) of the distribution. Figure 8*A* illustrates schematically a normally distributed set of synapses with SD of 0.5 mm and a peak density of 1.0 (Fig. 8*A*). Anatomic variations might occur in the peak density of synapses, keeping SD constant (Fig. 8*B*), or in SD, keeping peak density constant (Fig. 8*C*). Alternatively, the synapse distribution from a strip might be asymmetrical (Fig. 8*D*), but we have not modelled this. It should be noted that the synaptic connections underlying propagation patterns may be only a small subset of all horizontal connections.

We modeled the cortex as a series of vertical strips, each 60 μm wide. Either the amplitude (Fig. 9*A, left*; "Amp" varying from 0.1 to 1.0) or the SD (Fig. 9*B, right*; SD varying from 0.1 to 0.3 mm) of the synapse density function for each strip was varied as a simple sine function (with a period of 1 mm) of horizontal distance across the cortex. Propagation in a given direction was assumed to depend only on those synapses projecting in that direction, so only half of the synapse distribution from each strip was considered, and the Figure (Fig. 9*A*) reflects this. The cumulative density of synapses at each horizontal position was then calculated numerically, and the resulting distribution was smoothed, the peaks normalized to 1.0 and plotted. Both types of variations gave a periodic distribution of synapses across the cortex; varying amplitude yielded a nearly sinusoidal distribution (Fig. 9*B, left*), whereas varying SD yielded a more complex, skewed pattern (Fig. 9*B, right*).

When the same amplitude distribution is used to generate a cumulative density distribution for synapses projecting in the opposite direction across cortex (Fig. 9*C, left; dashed line*), the two synapse distributions are 180° out of phase (Fig. 9*C, left*; compare *thin solid* and *dashed lines*). Similarly, the sine function used to vary SD also yields essentially phase-inverted cumulative density patterns for the two directions (Fig. 9*C, right*; compare *thin solid* and *dashed lines*).

Consideration of some physiological properties of cortex and PFPs lead us to suggest that the periodic, directionally phase-inverted patterns of synapse density exemplified by our model could yield periodic, directionally phase-inverted patterns of PFP propagation. Specifically, *1*) action-potential conduction along intracortical axons is relatively fast; estimates range from ~0.3 to 32 m/s (34, 46). In contrast the PFP conduction velocity, averaged over millimeters, is well under 0.1 m/s. *2*) PFP duration, and thus the sustained firing of neurons recruited into the epileptiform event, is much longer than the PFP propagation time across even the longest of horizontal connections. *3*) Each PFP is also followed by a long absolute refractory period, which eliminates backward propagation. *4*) We assume that the rate-limiting step in propagation is the time necessary for excitation of local populations of neurons to build up to, and generate, a local synchronized event (i.e., the PFP), and the speed with which a local population generates a PFP is proportional to the total number of synapses activating it (cf. Ref. 44).

The quantitative association between synapse density and pattern, and PFP propagation is, of course, unknown. The property of phase-inversion in particular might be sensitive to these specifics. However, it is likely that regions of highest synapse density would reach PFP threshold fastest, and thus support the fastest PFP propagation. Our model suggests that rat SmI and cat area 17 may have systematic variations, with an average period of roughly 1 mm, in either the absolute density or the degree of spread (or both) with which synapses project horizontally. Horizontal projections from a single column of neurons need not be asymmetrical; directionality might arise from periodic variations in projection densities *between* neighboring columns. The model predicts that the reciprocal innervation of adjacent columns of cortex will often be strongly asymmetrical.

This model cannot account for the observation that the PFP sometimes skips over a small region of cortex, nor for the directionality of skipping. Such behavior would necessarily require that some axons project horizontally over a relatively long distance while making few synapses within an intervening region. Anatomically demonstrated interpatch distances (schematized in Fig. 8*E*) are similar to the periodicity of PFP propagation. Long-distance, patchy connections could excite a distant set of neurons before the nearer, adjacent neurons reached PFP threshold. Shorter, nonpatchy connections would allow the PFP to fill in the gaps at longer latencies. In principle, patchy connections alone might account for the periodic nature of propagation, or they might alter or promote the patterns described by our model.

In this effort to dissect the problem of propagation, both our experiments and the model designed to simulate them have neglected the role of synaptic inhibition. However, it seems likely that inhibition is an important factor in the behavior of clinical seizures. Focal application of GABA to the bicuculline-treated neocortical slice can delay or terminate a propagating PFP (6). Also, when slices are bathed in very low doses of bicuculline, which only partially block synaptic inhibition, the forms of PFP initiation and propagation are very different from those reported here (4). Another potential factor in the pattern of PFP propagation is the spatial variation of intrinsic excitability of the cortical neurons, or subset of neurons, that is critical to the initiation of the PFP, or perhaps variation in the local density of these neurons (7, 17, 31). The spread of epileptiform activity through the cortex may ultimately depend upon interactions between intrinsic excitatory and inhibitory connections, neuronal excitability, and the extrinsic factors that modulate them.

ACKNOWLEDGMENTS

We thank A. Agmon, Y. Chagnac-Amitai, and L. Silva for helpful discussions and comments on the manuscript; K. L. Chow for expert histological consultations; and G. Dennison for technical assistance.

R. D. Chervin was supported by a Kevin Walton Fellowship from Stanford University and a Medical Student Fellowship from the Epilepsy Foundation of America.

P. A. Pierce was supported by the Epilepsy Training Program of the Department of Neurology (NS-07280 from the National Institutes of Health). The following grants to B. W. Connors also supported this work: a fellowship from the Klingenstein Fund and NIH Grants NS-12151 and NS-01016.

Present address of B. W. Connors: Section of Neurobiology, Box G, Division of Biology & Medicine, Brown University, Providence, RI 02912.

Received 5 February 1988; accepted in final form 13 June 1988.

REFERENCES

1. AKERS, R. M. AND KILLACKEY, H. P. Organization of corticocortical connections in the parietal cortex of the rat. *J. Comp. Neurol.* 181: 513–538, 1978.
2. ASANUMA, H. AND ROSEN, I. Spread of mono- and polysynaptic connections within cat's motor cortex. *Exp. Brain Res.* 16: 507–520, 1973.
3. BLASDEL, G. G., LUND, J. S., AND FITZPATRICK, D. Intrinsic connections of macaque striate cortex: axonal projections of cells outside lamina 4C. *J. Neurosci.* 5: 3350–3369, 1985.
4. CHAGNAC-AMITAI, Y. AND CONNORS, B. W. Initiation and spread of synchronized neuronal activity in neocortex during partial blockade of synaptic inhibition. *Soc. Neurosci. Abstr.* 13: 1155, 1987.
5. CHAPIN, J. K., SADEQ, M., AND GUISE, J. L. U. Corticocortical connections within the primary somatosensory cortex of the rat. *J. Comp. Neurol.* 263: 326–346, 1987.
6. CHERVIN, R. D. AND CONNORS, B. W. Lateral propagation of synchronized paroxysmal discharges in the disinhibited neocortex. *Soc. Neurosci. Abstr.* 12: 350, 1986.
7. CONNORS, B. W. Initiation of synchronized neuronal bursting in neocortex. *Nature Lond.* 310: 685–687, 1984.
8. CONNORS, B. W. AND CHERVIN, R. D. Physiological evidence for periodicity and directionality of lateral excitatory connections in rat neocortex. *Soc. Neurosci. Abstr.* 12: 350, 1986.
9. CONNORS, B. W., GUTNICK, M. J., AND PRINCE, D. A. Electrophysiological properties of neocortical neurons in vitro. *J. Neurophysiol.* 48: 1302–1320, 1982.
10. CONNORS, B. W., MALENKA, R. C., AND SILVA, L. R. Inhibition of neocortical pyramidal neurones in rat and cat: two types of postsynaptic potentials, and $GABA_A$ and $GABA_B$ receptor-mediated responses. *J. Physiol. Lond.* In press.
11. DONOGHUE, J. P. AND WISE, S. P. The motor cortex of the rat: cytoarchitecture and microstimulation mapping. *J. Comp. Neurol.* 212: 76–88, 1982.
12. DRAGER, U. C. Receptive fields of single cells and topography in mouse visual cortex. *J. Comp. Neurol.* 160: 269–290, 1975.
13. EBERSOLE, J. S. AND CHATT, A. Spread and arrest of seizures: the importance of layer 4 in laminar interactions during neocortical epileptogenesis. *Advances in Neurology, Basic Mechanisms of the Epilepsies*, edited by A. V. Delgado-Escueta, et al. 1986, vol. 44, p. 515–558.
14. GABBOTT, P. L. A., MARTIN, K. A. C., AND WHITTERIDGE, D. Connections between pyramidal neurons in layer 5 of cat visual cortex (area 17). *J. Comp. Neurol.* 259: 364–381, 1987.
15. GILBERT, C. D. AND WEISEL, T. N. Clustered intrinsic connections in cat visual cortex. *J. Neurosci.* 3: 1116–1133, 1983.
16. GOLDENSOHN, E. S. AND SALAZAR, A. M. Temporal and spatial distribution of intracellular potentials during generation and spread of epileptogenic discharges. *Advances in Neurology, Basic Mechanisms of the Epilepsies*, edited by A. V. Delgado-Escueta, et al. 1986, vol. 44, p. 559–582.
17. GUTNICK, M. J., CONNORS, B. W., AND PRINCE, D. A. Mechanisms of neocortical epileptogenesis in vitro. *J. Neurophysiol.* 48: 1321–1335, 1982.
18. GUTNICK, M. J. AND WADMAN, W. J. Intrinsic neuronal connectivity in neocortical brain slices as revealed by non-uniform propagation of paroxysmal discharges. *Soc. Neurosci. Abstr.* 12: 349, 1986.
19. HUBEL, D. H. AND WIESEL, T. N. Shape and arrangement of columns in cat's striate cortex. *J. Physiol. Lond.* 165: 559–568, 1963.
20. ISSEROFF, A., SCHWARZ, M. L., DEKKER, J. J., AND GOLDMAN-RAKIC, P. S. Columnar organization of callosal and associational projections from rat frontal cortex. *Brain Res.* 293: 213–223, 1984.
21. JASPER, H. H. Mechanisms of propagation: extracellular studies. In: *Basic Mechanisms of the Epilepsies*. Boston, MA: Little, Brown, 1969, p. 421–438.
22. KISVARDY, Z. F., MARTIN, K. A. C., FREUND, T. F., MAGLOCZKY, ZS., WHITTERIDGE, D., AND SOMOGYI, P. Synaptic targets of HRP-filled layer II pyramidal cells in cat striate cortex. *Exp. Brain Res.* 64: 541–552, 1986.
23. KNOWLES, W. D., TRAUB, R. D., AND STROWBRIDGE, B. W. The initiation and spread of epileptiform bursts in the in vitro hippocampal slice. *Neuroscience* 21: 441–455, 1987.
24. LEMIEUX, J. F. AND BLUME, W. T. Topographical evolution of spike-wave complexes. *Brain Res.* 373: 275–287, 1986.
25. LOWEL, S., FREEMAN, B., AND SINGER, W. Topographic organization of the orientation column system in large flat-mounts of the cat visual cortex. A 2-deoxyglucose study. *J. Comp. Neurol.* 255: 401–415, 1987.
26. LOWEL, S. AND SINGER, W. The pattern of ocular dominance columns in flat-mounts of the cat visual cortex. *Exp. Brain Res.* 68: 661–666, 1987.
27. LUHMANN, H. L., MARTINEZ MILLAN, L., AND SINGER, W. Development of horizontal intrinsic connections in cat striate cortex. *Exp. Brain Res.* 63: 443–448, 1986.
28. MARTIN, K. A. C. Neuronal circuits in cat striate cortex. In: *Cerebral Cortex, Functional Properties of Cortical Cells*. New York: Plenum, 1984, vol. 2, p. 241–284.
29. MARTIN, K. A. C. AND WHITTERIDGE, D. Form, function and intracortical projections of spiny neu-

rones in the striate visual cortex of the cat. *J. Physiol. Lond.* 353: 463–504, 1984.
30. MATSUBARA, J., CYNADER, M., SWINDALE, N. V., AND STRYKER, M. P. Intrinsic projections within visual cortex: evidence for orientation-specific local connections. *Proc. Natl. Acad. Sci. USA* 82: 935–939, 1985.
31. MCCORMICK, D. A., CONNORS, B. W., LIGHTHALL, J. W., AND PRINCE, D. A. Comparative electrophysiology of pyramidal and sparsely spiny stellate neurons of the neocortex. *J. Neurophysiol.* 54: 782–806, 1985.
32. MCGUIRE, B. A., GILBERT, C. D., AND WEISEL, T. N. Ultrastructural characterization of long-ranged clustered horizontal connections in monkey striate cortex. *Soc. Neurosci. Abstr.* 11: 17, 1985.
33. MILES, R. AND WONG, R. K. S. Excitatory synaptic interactions between CA3 neurons in the guinea pig hippocampus in vitro. *J. Physiol. Lond.* 373: 397–418, 1986.
34. MITANI, A. AND SHIMOKOUCHI, M. Neuronal connections in the primary auditory cortex: an electrophysiological study in the cat. *J. Comp. Neurol.* 235: 417, 1985.
35. PETSCHE, H., PROHASKA, O., RAPPELSBERGER, P., VOLLMER, R., AND KAISER, A. Cortical seizure patterns in multidimensional view: the information content of equipotential maps. *Epilepsia* 15: 439–463, 1974.
36. PRINCE, D. A. Neurophysiology of epilepsy. *Ann. Rev. Neurosci.* 1: 395–415, 1978.
37. ROCKLAND, K. S. AND LUND, J. S. Intrinsic laminar lattice connections in primate visual cortex. *J. Comp. Neurol.* 216: 303–318, 1983.
38. ROCKLAND, K. S., LUND, J. S., AND HUMPHREY, A. L. Anatomical banding of intrinsic connections in striate cortex of tree shrews. *J. Comp. Neurol.* 209: 41–58, 1982.
39. SCHMITT, F. O., WORDEN, F. G., ADELMAN, G., AND DENNIS, S. G. *The Organization of Cerebral Cortex.* Cambridge, MA: MIT Press, 1981.
40. SHATZ, C. J., LINDSTROM, S., AND WIESEL, T. N. The distribution of afferents representing the right and left eyes in the cat's visual cortex. *Brain Res.* 131: 103–116, 1977.
41. SHAW, C., YINON, U., AND AUERBACH, E. Receptive fields and response properties of neurons in rat visual cortex. *Vision Res.* 15: 203–208, 1975.
42. SILVA, L. R. AND CONNORS, B. W. Spatial distribution of intrinsic cortical neurons that excite or inhibit layer 2/3 pyramidal cells: a physiological study of neocortex in vitro. *Soc. Neurosci. Abstr.* 12: 1453, 1986.
43. TRAUB, R. D., KNOWLES, W. D., MILES, R., AND WONG, R. K. S. Models of the cellular mechanism underlying propagation of epileptiform activity in the CA2-CA3 region of the hippocampal slice. *Neuroscience* 21: 457–470, 1987.
44. TRAUB, R. D., MILES, R., AND WONG, R. K. S. Models of synchronized hippocampal bursts in the presence of inhibition. I. Single population events. *J. Neurophysiol.* 58: 739–751, 1987.
45. TS'O, D. Y., GILBERT, C. D., AND WIESEL, T. N. Relationships between horizontal interactions and functional architecture in cat striate cortex as revealed by cross correlation analysis. *J. Neurosci.* 6: 1160–1170, 1986.
46. WAXMAN, S. G. AND SWADLOW, H. A. The conduction properties of axons in central white matter. *Prog. Neurobiol.* 8: 297–324, 1977.
47. WELKER, C. AND WOOLSEY, T. A. Structure of layer IV in the somatosensory neocortex of the rat: description and comparison with the mouse. *J. Comp. Neurol.* 158: 437–454, 1976.
48. WIESENFELD, Z. AND KORNEL, E. E. Receptive fields of single cells in the visual cortex of the hooded rat. *Brain Res.* 94: 401–412, 1975.
49. WYLER, A. R. AND WARD, A. A. Neuronal firing patterns from epileptogenic foci of monkey and human. *Advances in Neurology, Basic Mechanisms of the Epilepsies,* edited by A. V. Delgado-Escueta, et al. 1986, vol. 44, p. 967–989.
50. YAARI, Y., KONNERTH, A., AND HEINEMANN, U. Spontaneous epileptiform activity of CA1 hippocampal neurons in low extracellular calcium solutions. *Exp. Brain Res.* 51: 153–156, 1983.
51. ZILLES, K., WREE, A., SCHLEICHER, A. AND DEVAC, I. The monocular and binocular subfields of rat's primary visual cortex. A quantitative morphological approach. *J. Comp. Neurol.* 226: 391–402, 1984.